Cancer Research

Api6/AIM/Spα/CD5L Overexpression in Alveolar Type II Epithelial Cells Induces Spontaneous Lung Adenocarcinoma

Yuan Li[1,2,3,4], Peng Qu[1,2,3], Lingyan Wu[1,2,3], Beilin Li[1,2,3], Hong Du[3], and Cong Yan[1,2,3]

Abstract

Chronic inflammation is an important contributor to the development of lung cancers, one of the most common malignancies worldwide, but the underlying molecular mechanisms of inflammation that specifically cue cancer risk remain poorly understood. Apoptosis inhibitor 6 (Api6, also known as AIM, Sp-α, and CD5L) is a downstream target gene of neutral lipids and peroxisome proliferator–activated receptor gamma in lung alveolar type II (AT II) epithelial cells. An association among increased expression of Api6 in certain settings of pathogenic lung inflammation in mice prompted us to hypothesize a possible role in cancer. Here, we report that Api6 promotes malignant transformation by limiting lung epithelial cell apoptosis and promoting immune escape. The specific function of Api6 in AT II cells was determined by using a doxycycline-inducible Api6 mouse model. Api6 overexpression inhibited apoptosis and activated oncogenic signaling in AT II lung epithelial cells, inducing emphysema and adenocarcinoma. In addition, Api6 overexpression in AT II cells increased the concentrations of proinflammatory cytokines/chemokines in bronchoalveolar lavage fluid and serum, promoting expansion of myeloid-derived suppressor cells (MDSC) in lung and blood but not in bone marrow or spleen. Lung MDSCs suppressed T-cell proliferation and activity *in vitro* and reduced levels of T cells *in vivo* following doxycycline treatment to activate Api6. Together, our findings establish that Api6 promotes lung tumorigenesis by blocking a mechanism of epithelial apoptosis that would normally support immunosurveillance. *Cancer Res; 71(16); 5488–99. ©2011 AACR.*

Introduction

Neutral lipid metabolism plays an important role in maintaining tissue homeostasis and controlling inflammation. We have previously found that blocking neutral lipid metabolism in lysosomal acid lipase (LAL, EC 3.1.1.13) knockout mice ($lal^{-/-}$) leads to severe tissue inflammation and diseases in multiple organs, including the lung (1–6). LAL converts cholesterol ester and triglycerides to free cholesterol and free fatty acids. In an effort to identify downstream target genes of LAL to promote lung inflammation, we previously reported that apoptosis inhibitor 6 (Api6, also known as AIM, Sp-α, and CD5L) expression was increased 70-folds in the $lal^{-/-}$ lung by Affymetrix GeneChip microarray analysis (3, 4). Api6 is a secreted protein and it belongs to the macrophage scavenger receptor cysteine-rich domain superfamily (SRCR-SF; refs. 7, 8). It has been reported that Api6 inhibits fatty acid synthase activity (9).

In the lung, aberrant upregulation of Api6 occurs primarily in alveolar type II (AT II) epithelial cells of $lal^{-/-}$ mice (4). AT II epithelial cells can serve as regional immune cells that synthesize/secrete proinflammatory cytokines/chemokines to recruit inflammatory cells into the lung in favor of tumor initiation and growth (10, 11). AT II epithelial cells are regional tumor progenitor cells (10, 11). To determine the functional role of Api6 in AT II epithelial cells, an epithelial-specific CCSP-rtTA/$(TetO)_7$-CMV-Api6 bitransgenic mouse model has been generated. This report shows that Api6 is a proinflammatory and oncogenic molecule. Overexpression of Api6 in AT II epithelial cells promotes spontaneous emphysema and adenocarcinoma in the lung by blocking epithelial apoptosis to promote cancerous transformation and inhibiting immune surveillance. In humans, expression of the Api6 gene is upregulated in chronic obstructive pulmonary disease (COPD; the major phenotype is emphysema) and lung cancer.

Materials and Methods

Animal care

All scientific protocols involving the use of animals in this study have been approved by the Institution Animal Care and

Authors' Affiliations: [1]The Center for Immunobiology, [2]IU Simon Cancer Center, [3]Department of Pathology and Laboratory Medicine, Indiana University School of Medicine, Indianapolis, Indiana; and [4]Cancer Center, Departments of Pathology and Oncology, Shanghai Medical College, Fudan University, Shanghai, China

Note: Supplementary data for this article are available at Cancer Research Online (http://cancerres.aacrjournals.org/).

Y. Li and P. Qu contributed equally to this work.

Corresponding Author: Cong Yan, Department of Pathology and Laboratory Medicine, Indiana University School of Medicine, 980 W. Walnut Street, Walther Hall C418, Indianapolis, IN 46202-5188. Phone: 317-278-6005; Fax: 317-278-7030; E-mail: coyan@iupui.edu or Hong Du, Department of Pathology and Laboratory Medicine, Indiana University School of Medicine, VanNuys Medical Science Building, Room A132, 635 Barnhill Drive, Indianapolis, IN 46202. Phone: 317-274-6535; Fax: 317-278-2018; E-mail: hongdu@iupui.edu

doi: 10.1158/0008-5472.CAN-10-4225

Usage Committee (IACUC) of Indiana University School of Medicine, and follow the guidelines established by the Panel on Euthanasia of the American Veterinary Medical Association. Protocols involving the use of recombinant DNA or biohazardous materials have been approved by the Institutional Biosafety Committee and follow the guidelines established by the NIH. Animals were housed under IACUC-approved conditions in a secure animal facility at Indiana University School of Medicine. Animals were regularly screened for common pathogens. Experiments involving animal sacrifice utilize CO_2 narcosis to minimize animal discomfort.

Generation of doxycycline-controlled Api6 transgenic mice

Previously made $(TetO)_7$-CMV-Api6 (12) and CCSP-rtTA (13) single transgenic mouse lines were crossbred to generate CCSP-rtTA/$(TetO)_7$-CMV-Api6 bitransgenic mouse line.

Lung histology and morphometry

The trachea was cannulated and the cannula was tied firmly in place. The lungs were filled through the trachea with 4% paraformaldehyde in PBS at 20 cm H_2O pressure by gravity and maintained overnight at 4°C. The lungs were monitored for leakage during this procedure at 4°C for approximately 24 hours, and only lungs that did not leak were used for further study. The lungs were washed with PBS and dehydrated through a series of ethanol followed by paraffin embedding. Sections (5 μm) were mounted on glass slides and deparaffinized. The adult lung slides were washed in a series of xylene and ethanol to remove paraffin from the tissues. Multiple sections from each lung were stained with hematoxylin and eosin (H&E). For quantitative characterization, the images (20×) were transferred by video camera to a computer screen. The measurements of alveolar number, alveolar sphere surface area, and alveolar volume were determined by MetaMorph imaging software. Twenty randomly selected microscopic focal emphysema fields were analyzed.

Reverse transcription and real-time PCR

As described previously (10), all reverse transcription reactions were set up by the Taqman Reverse Transcription Kit (Applied Biosystems).

$CD11b^+Ly6G^+$ cell immune suppressive assay

$CD11b^+Ly6G^+$ cells were isolated from the lung of wild-type, doxycycline-treated or untreated bitransgenic mice as described previously (11).

ELISA for cytokine analysis

The protein levels of cytokines and lymphokines [interleukin-2 (IL-2), IL-4, and IFN-γ] in bronchoalveolar lavage fluid (BALF), blood serum, and culture medium were measured by DueSet ELISA kits (R&D Systems).

Fluorescence-activated cell sorting analysis

Cells were isolated from the bone marrow, spleen, blood, and lung and analyzed by fluorescence-activated cell sorting (FACS) as previously described (11, 14). To measure intracellular signaling molecules, a previous procedure was followed by using cell surface markers and phospho-specific antibodies followed by FACS analysis (6).

Conversion of alveolar macrophages to myeloid-derived suppressor cells *in vitro*

Alveolar macrophages were isolated from BALF as described previously (3). Isolated macrophages were cultured in RPMI 1640 medium with or without 100 ng/mL Api6 (R&D Systems) for 2 days. FACS and ELISA analyses were carried out as outlined above.

Caspase-3 activity assay

Caspase-3 activity was measured by ApoAlert assay kit (BD Biosciences Clonetech). Cells from the whole lung, AT II epithelial cells, and alveolar macrophages of 3-month doxycycline-treated or untreated bitransgenic mice were washed twice with cold PBS and lysed on ice in 50 μL lysis buffer. Cell lysates were centrifuged at 13,000 rpm for 10 minutes to remove cellular debris. Each assay was conducted in triplicates in a 96-well plate based on the manufacturer's protocol. Plates were read (excitation 360 nmol/L; emission 480 nmol/L) by using a Spectra max Gemini XPS (Molecular Devices) multiwell fluorescence plate reader. A minimum of 3 experiments were carried out for each sample.

Apoptosis by Annexin V assay

A previous procedure was followed (14).

Bromodeoxyuridine assay

A previous procedure was followed (12).

Statistical analysis

A paired Student's *t* test or ANOVA was used to evaluate the significance of the differences. Statistical significance was set at $P < 0.05$.

Results

Generation of CCSP-rtTA/$(TetO)_7$-CMV-Api6 bitransgenic mice

A previously made CCSP-rtTA transgenic mouse line (13) was crossbred with a previously generated $(TetO)_7$-CMV-Api6 transgenic mouse line (ref. 12; Fig. 1A). A Flag sequence was inserted at the C terminus of Api6 cDNA to distinguish it from endogenous Api6. Single transgenic and bitransgenic mice were detected by PCR, using sequence-specific primers for transgene constructs (Fig. 1B). After doxycycline treatment, the Api6 mRNA level was highly induced in AT II epithelial cells of bitransgenic mice compared with those of untreated mice (Fig. 1C). The Api6 mRNA level was not induced in AT II epithelial cells of CCSP-rtTA and $(TetO)_7$-CMV-Api6 single transgenic mice regardless of doxycycline treatment. Furthermore, FACS analysis showed induced expression of the Api6-Flag fusion protein in AT II epithelial cells when costained with Flag antibody and SP-C antibody (AT II cell marker) in doxycycline-treated bitransgenic mice (Fig. 1D). No Api6-Flag

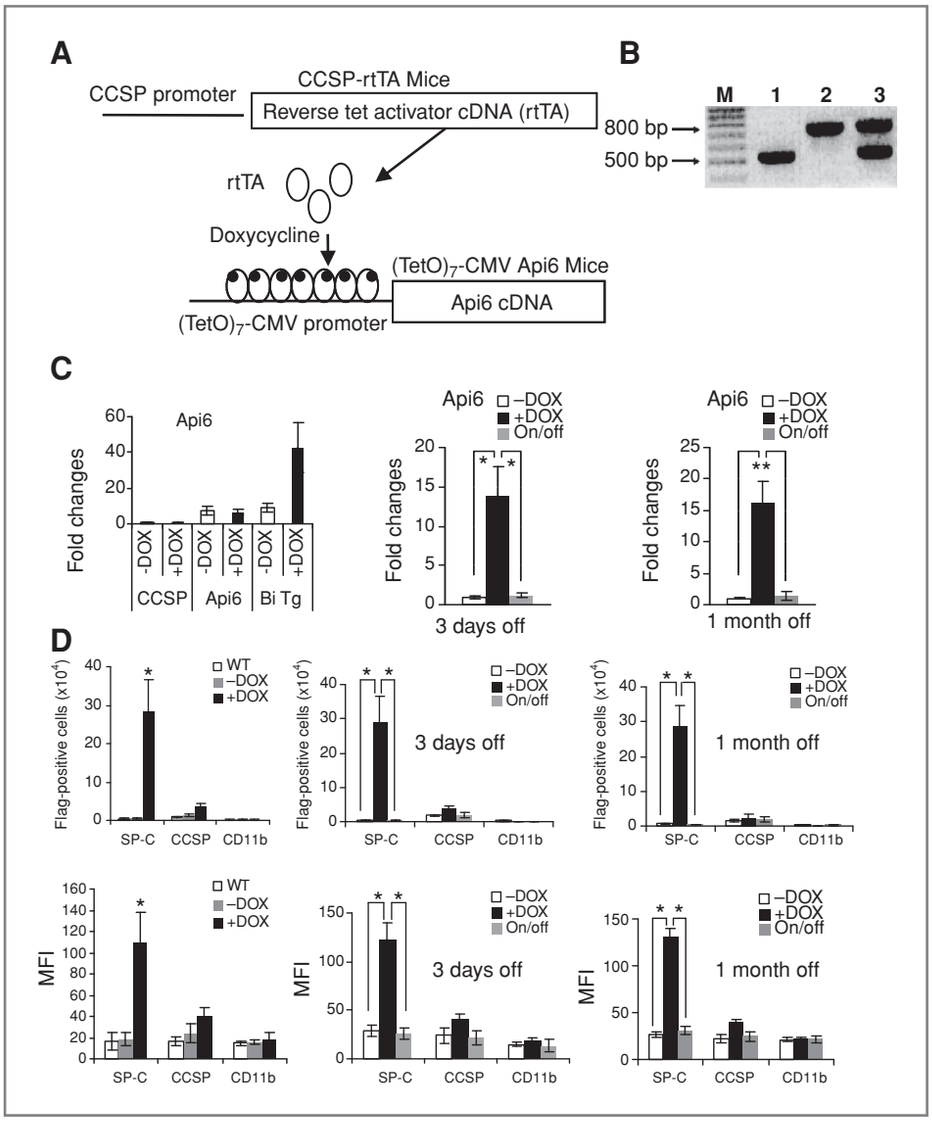

Figure 1. Generation of doxycycline-controlled CCSP-rtTA/(TetO)7-CMV-Api6 bitransgenic mice. A, illustration of the CCSP-rtTA/(TetO)7-CMV-Api6 bitransgenic mouse system. B, genotyping of CCSP-rtTA transgenic (lane 1), $(TetO)_7$-CMV-Api6 transgenic (lane 2), and CCSP-rtTA/$(TetO)_7$-CMV-Api6 bitransgenic (lane 3) mice. The M lane is DNA ladder. C, real-time PCR to quantify mRNA expression levels of Api6 in AT II epithelial cells of CCSP-rtTA single transgenic mice (CCSP), $(TetO)_7$-CMV-Api6 single transgenic mice (Api6), and CCSP-rtTA/$(TetO)_7$-CMV-Api6 bitransgenic mice (Bi Tg) that were treated (+DOX) or untreated (−DOX) with doxycycline for 3 months. The numbers were normalized by glyceraldehyde-3-phosphate dehydrogenase (GAPDH) mRNA expression. In separate groups, doxycycline was removed for 3 days or 1 month from bitransgenic mice followed by real-time PCR analysis of Api6 mRNA expression. Results represent the mean ± SD. $n = 3$ to 5, *, $P < 0.05$. D, expression levels of Api6-Flag fusion protein in bitransgenic mice. Lung single cells from 3-month +DOX or −DOX CCSP-rtTA/$(TetO)_7$-CMV-Api6 bitransgenic mice or wild-type mice (WT) were labeled with anti-Flag antibody and cell surface marker anti–SP-C antibody (AT II epithelial cell marker) or anti-CCSP antibody (Clara cell marker) or anti-CD11b antibody (macrophage marker) and analyzed by FACS. Isotype antibodies were used as control. In separate groups, doxycycline was removed for 3 days or 1 month from bitransgenic mice followed by FACS analysis of Api6 protein expression. Results represent the mean ± SD. $n = 3$ to 5, *, $P < 0.05$. MFI, mean fluorescence intensity.

fusion protein was detected in Clara cells and alveolar macrophages when costained with Flag antibody and CCSP (Clara cell marker) or CD11b antibody (macrophage marker) regardless of doxycycline treatment. Selective expression of reporter gene in CCSP-rtTA transgenic system in AT-II epithelial cells has been previously reported (13). In wild-type mice, no Api6-Flag fusion protein was observed in AT II epithelial cells regardless of doxycycline treatment except nonspecific signals. Both the Api6 mRNA and protein levels in doxycycline-treated bitransgenic mice were reduced to the basal level after doxycycline removal for 3 days or 1 month (Fig. 1C and D).

Overexpression of Api6 inhibited apoptosis in the lung of CCSP-rtTA/$(TetO)_7$-CMV-Api6 bitransgenic mice

To assess whether Api6 overexpression alters the apoptotic activity in AT II epithelial cells, whole lung cells were isolated

from doxycycline-treated or untreated bitransgenic mice, and labeled with Annexin V and fluorochrome-conjugated anti–SP-C antibodies. FACS analysis showed a more than 7-fold decrease of Annexin V–labeled AT II epithelial cells in 3-month doxycycline-treated bitransgenic mice compared with untreated littermates (Fig. 2A). Api6 also stimulated proliferation of AT II epithelial cells in doxycycline-treated bitransgenic mice (Fig. 2A). As a consequence, SP-C$^+$ epithelial cells were significantly increased in doxycycline-treated bitransgenic mice (Fig. 2A). In addition, mRNA expression levels of proapoptotic genes (*Bad*, *CideA*, *Casp3*, *Casp7*, *Casp9*, *Apaf-1*, and *FasL*) in AT II epithelial cells were significantly decreased compared with those of untreated bitransgenic mice as assessed by real-time PCR. Some of these genes also showed decreased expression levels in alveolar macrophages and whole lungs (Fig. 2B). Furthermore, the caspase-3 activity in cell lysates that were isolated from whole lung cells, AT II epithelial cells, and alveolar macrophages of 3-month doxycycline-treated bitransgenic mice was decreased compared with that in untreated bitransgenic mice (Fig. 2C). These

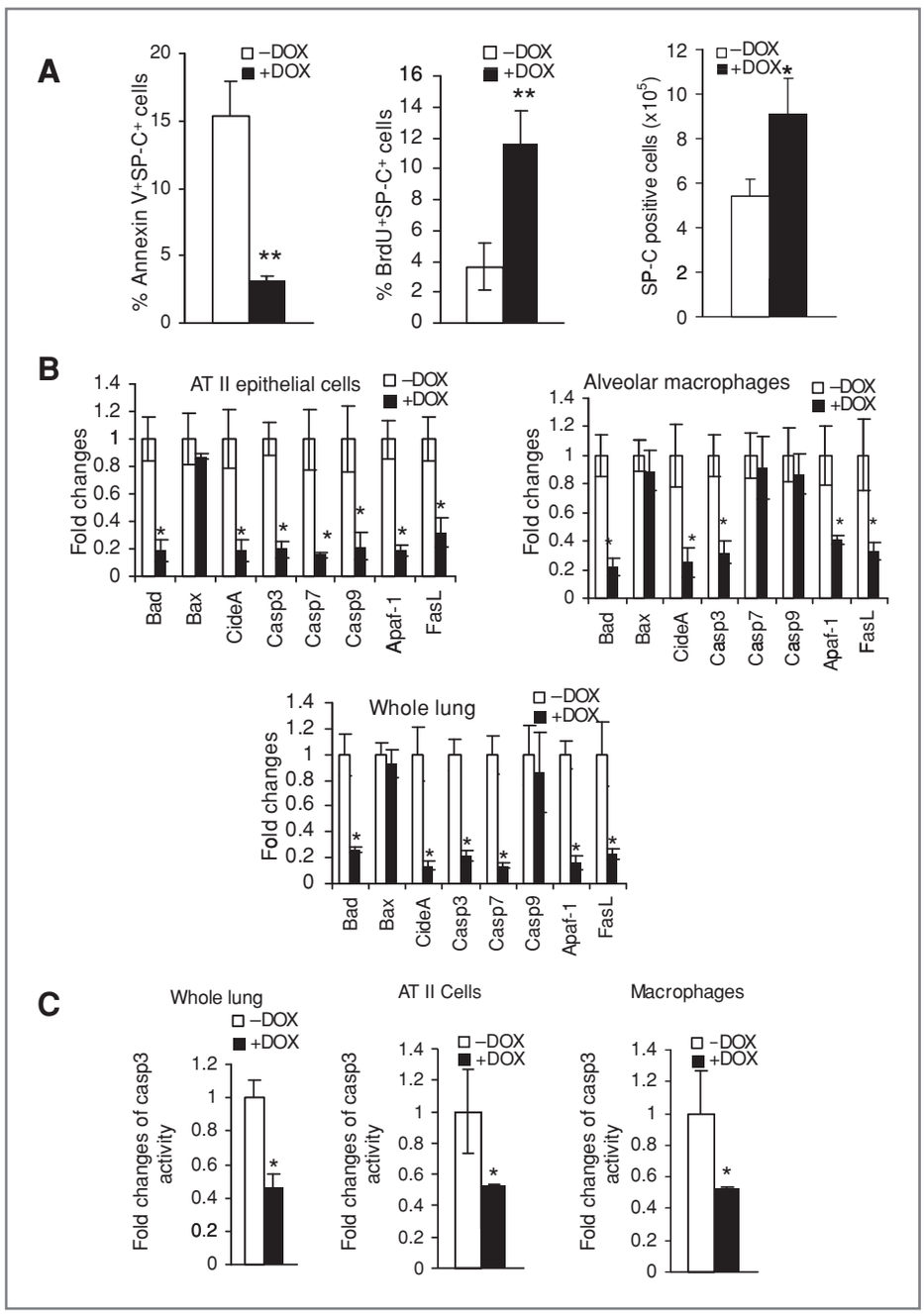

Figure 2. Apoptosis inhibition in the lung of bitransgenic mice. A, lung single cells from 3-month doxycycline-treated (+DOX) or untreated (−DOX) bitransgenic mice were stained with anti–SP-C antibody (AT II epithelial cell marker) and Annexin V or bromodeoxyuridine (BrdU) antibodies for FACS analysis. Results represent the mean ± SD from 3 independent experiments ($n = 3$). *, $P < 0.05$; **, $P < 0.01$. B, real-time PCR was carried out to quantify mRNA expression levels of apoptotic molecules in AT II epithelial cells, alveolar macrophages, and whole lung of 3-month +DOX or −DOX bitransgenic mice and normalized by GAPDH mRNA expression. Results represent the mean ± SD from 5 independent experiments ($n = 5$). *, $P < 0.05$. C, the caspase-3 activity was measured in cell lysates containing equivalent amount of proteins from whole lung, AT II epithelial cells, and alveolar macrophages of 3-month +DOX or −DOX bitransgenic mice in triplicates. Results represent the mean ± SD from 3 independent experiments ($n = 3$). *, $P < 0.05$.

studies suggest that Api6 was able to inhibit apoptosis in lung epithelial cells and alveolar macrophages in autocrine and paracrine fashions. When doxycycline was removed from the treated mice for 3 days, Annexin V activity and expression of apoptotic genes did not revert to the normal levels in the lung (Supplementary Fig. S1A and B). Even when doxycycline was removed for 1 month, the Annexin V activity, expression of most apoptotic genes, and cell proliferation were not completely recovered to the normal levels in the lung (Supplementary Fig. S2A and B).

Overexpression of Api6 induced emphysema and adenocarcinoma in the lung of CCSP-rtTA/$(TetO)_7$-CMV-Api6 bitransgenic mice

To evaluate the pathogenic consequence of Api6 overexpression in the lung, bitransgenic mice were treated with doxycycline for various time lengths. Histopathologic analyses revealed coexistence of emphysema and hypercellularity in the lung after 6 weeks of doxycycline treatment (Fig. 3A, *+DOX* 6w). Quantitative analysis showed that alveolar numbers of doxycycline-treated bitransgenic mice in focal

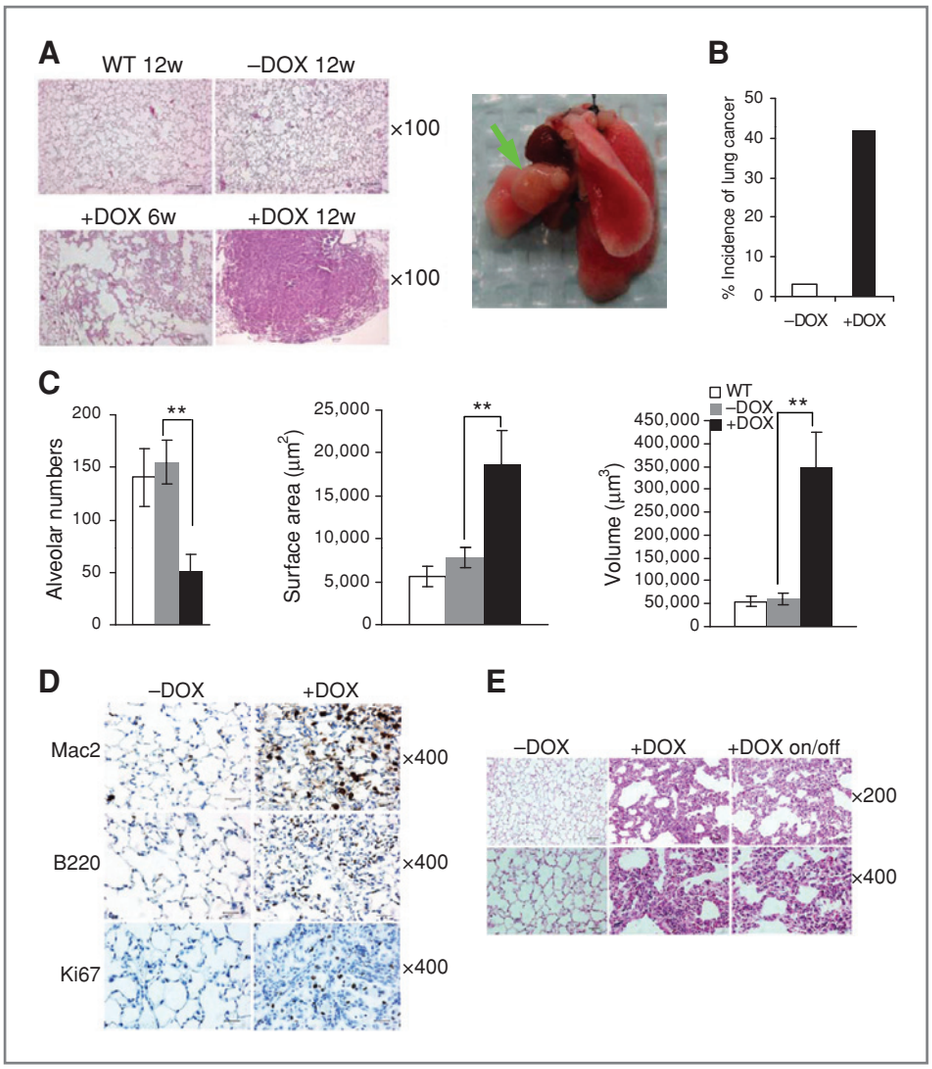

Figure 3. Api6 overexpression caused emphysema and adenocarcinoma in the lung of bitransgenic mice. A, histologic analysis of doxycycline-treated (+DOX) or untreated (−DOX) bitransgenic mice at various time points by H&E staining. After 6 weeks of doxycycline treatment (+DOX 6w), emphysema and hyperplasia were observed. Adenocarcinomas were found in 12-week doxycycline-treated lungs (+DOX 12w), but not in age-matched untreated lungs (−DOX 12w). Normal lung tissue from 12-week wild-type mice (WT 12w) was used as control. A gross picture of lung tumor after 9 months of doxycycline treatment (pointed by the green arrow) was presented. B, the tumor incidence rates between 4 and 9 months of +DOX and −DOX bitransgenic mice ($n = 36$/group). C, quantitative measurements of alveolar number, alveolar surface area, and alveolar volume in +DOX and −DOX bitransgenic mice were determined by MetaMorph imaging software. Values are the mean ± SD, $n = 6$. **, $P < 0.01$. D, immunohistochemical staining with Mac2, B220, and Ki67 antibodies in 2-month +DOX and −DOX bitransgenic mice. E, doxycycline on/off study. Bitransgenic mice were treated with doxycycline for 2 months. One group of mice ($n = 5$) was terminated for treatment (+DOX on/off) and another group of mice ($n = 5$) continued to be treated (+DOX). One month later, mice were harvested, and the inflated lungs were stained with H&E. −DOX served as control.

emphysema areas were much less than those of untreated bitransgenic mice. The average alveolar sphere surface area and average alveolar volume were significantly increased in doxycycline-treated bitransgenic mice compared with those of untreated bitransgenic mice (Fig. 3C). Immunohistochemical staining identified infiltration of Mac2- and B220-positive inflammatory cells in the hyperplasia areas of 2-month doxycycline-treated bitransgenic mice prior to tumorigenesis, an indication of prior tumor inflammation (Fig. 3D). Twelve weeks after doxycycline treatment, adenocarcinomas as previously described (15) were observed in the lungs of bitransgenic mice (Fig. 3A, *+DOX 12*w). To determine the tumor incidence rate, bitransgenic mice were euthanized at 4 to 9 months after doxycycline treatment for histopathologic analyses. Of 36 doxycycline-treated bitransgenic mice, 15 mice developed lung tumors (41.67%; Fig. 3B). Four of them developed both pulmonary hyperplasia and adenocarcinoma. Eight of them developed adenocarcinoma. Three mice developed hyperplasia without adenocarcinoma. In most cases, one tumor per lung was observed. A few mice showed tumors on both sides of lung lobes. In comparison, only 1 mouse showed lung adenocarcinoma (3.03%) and another 1 developed pulmonary dysplasia without cancer in 33 doxycycline-untreated bitransgenic mice. None of the wild-type mice, CCSP-rtTA single transgenic mice, and $(TetO)_7$-CMV-Api6 single transgenic mice developed tumor or hyperplasia regardless of doxycycline treatment ($n = 10$). Finally, a doxycycline on/off experiment was carried out to assess whether the neoplastic process is reversible. Bitransgenic mice were treated with doxycycline for 2 months. One group of mice ($n = 5$) was terminated of doxycycline treatment, whereas another group of mice continued to be treated. Of the 5 deinduced mice, 3 developed hyperplasia 1 month later (Fig. 3E). It seems that removal of doxycycline did not stop the inflammation-induced neoplastic process. This is consistent with observations made in apoptosis, cell proliferation, and inflammatory analyses (Supplementary Figs. S1 and S2).

Overexpression of Api6 promoted proinflammatory microenvironment change in the lung of CCSP-rtTA/$(TetO)_7$-CMV-Api6 bitransgenic mice

Previously, we reported that persistent activation of the Stat3 pathway in AT II epithelial cells directly induced lung adenocarcinoma in CCSP-rtTA/$(TetO)_7$-CMV-Stat3C bitransgenic mice (10). This was the first animal model demonstrating that Stat3 activation is able to induce spontaneous tumor *in vivo*. To determine whether Stat3 was activated in AT II epithelial cells of CCSP-rtTA/$(TetO)_7$-CMV-Api6 bitransgenic mice as a part of the tumorigenic process, cells from whole lungs of 1-month doxycycline-treated or untreated bitransgenic mice were isolated and double labeled with fluorochrome-conjugated anti–phospho-Stat3Y705 and SP-C (AT II cell marker) antibodies. Labeled cells were analyzed by FACS. In gated SP-C–positive cells, the percentage of phospho-Stat3Y705 was dramatically increased in doxycycline-treated bitransgenic mice (16.16%) compared with that in untreated bitransgenic mice (3.62%; Supplementary Table S1). Other oncogenic intracellular molecules extracellular signal-regulated kinase (Erk) and P38 were significantly activated as well in doxycycline-treated bitransgenic mice. Akt was only activated in AT II epithelial cells, but not in lung myeloid-derived suppressor cells (MDSC). These observations suggest that Api6 overexpression was able to activate various oncogenic pathways in AT II epithelial cells to facilitate the neoplastic process. At the gene transcriptional level, Api6 overexpression stimulated mRNA expression of Stat3 and its upstream stimuli IL-6 in whole lung cells, AT II epithelial cells, and alveolar macrophages (Fig. 4A). Upregulation of IL-6 mRNA in the lung led to the increased concentration of secreted IL-6 in BALF and blood of 1-month doxycycline-treated bitransgenic mice compared with that in untreated bitransgenic mice as measured by ELISA (Fig. 4B and C). In addition, concentrations of IL-1β, IL-10, granulocyte macrophage–colony stimulating factor (GM-CSF), G-CSF, and VEGF were increased in BALF and blood of 1-month doxycycline-treated bitransgenic mice (Fig. 4B and C). It is well known that these factors play critical roles in recruiting and stimulating expansion of inflammatory cells (especially MDSCs) in inflammatory organs to exert immunosuppression in favor of tumor growth (16–18). Similar to that observed in the apoptotic studies, concentrations of these cytokines were not significantly decreased in BALF and plasma after 3 days of doxycycline removal (Supplementary Fig. S1C and D). When doxycycline was removed for 1 month, they were not completely reduced to the normal levels (Supplementary Fig. S2C and D).

Overexpression of Api6 stimulated expansion of MDSCs in the lung of CCSP-rtTA/$(TetO)_7$-CMV-Api6 bitransgenic mice

Because multiple MDSC-stimulating cytokines were increased in BALF and blood of bitransgenic mice after Api6 overexpression, it was important to determine expansion of MDSCs in the lung. Single-cell suspensions were prepared from the bone marrow, blood, spleen, and lung of 3-month doxycycline-treated, untreated bitransgenic mice, and age-matched wild-type mice. The percentage of $CD11b^+Ly6G^+$ myeloid cells were significantly increased in the blood (19.45%) and lung (31.99%) of doxycycline-treated mice compared with those (4.46% and 4.27%, respectively) in untreated bitransgenic mice. However, the percentage of $CD11b^+Ly6G^+$ myeloid cells in the bone marrow and spleen were relatively unchanged between doxycycline-treated and untreated bitransgenic mice (Fig. 5A). The total numbers of MDSCs in the lung were increased in a time-dependent fashion with a peak at 6 months of doxycycline treatment (Fig. 5B). Removal of doxycycline for 3 days and 1 month did not result in significant decreases in the total number of MDSCs in the lung (Fig. 5B). When phosphorylation of Stat3, Erk, and P38 was assessed in MDSCs, a similar observation was made. The phosphorylation levels of Stat3, Erk, and P38 in $CD11b^+Ly6G^+$ myeloid cells were significantly higher in the blood and lung, but not in the bone marrow and spleen of doxycycline-treated mice (Supplementary Table S1). Therefore, Api6 overexpression in lung epithelial cells only caused regional inflammation, not systemic inflammation. Because Api6 had no effect on bone marrow progenitor development, it is unlikely that

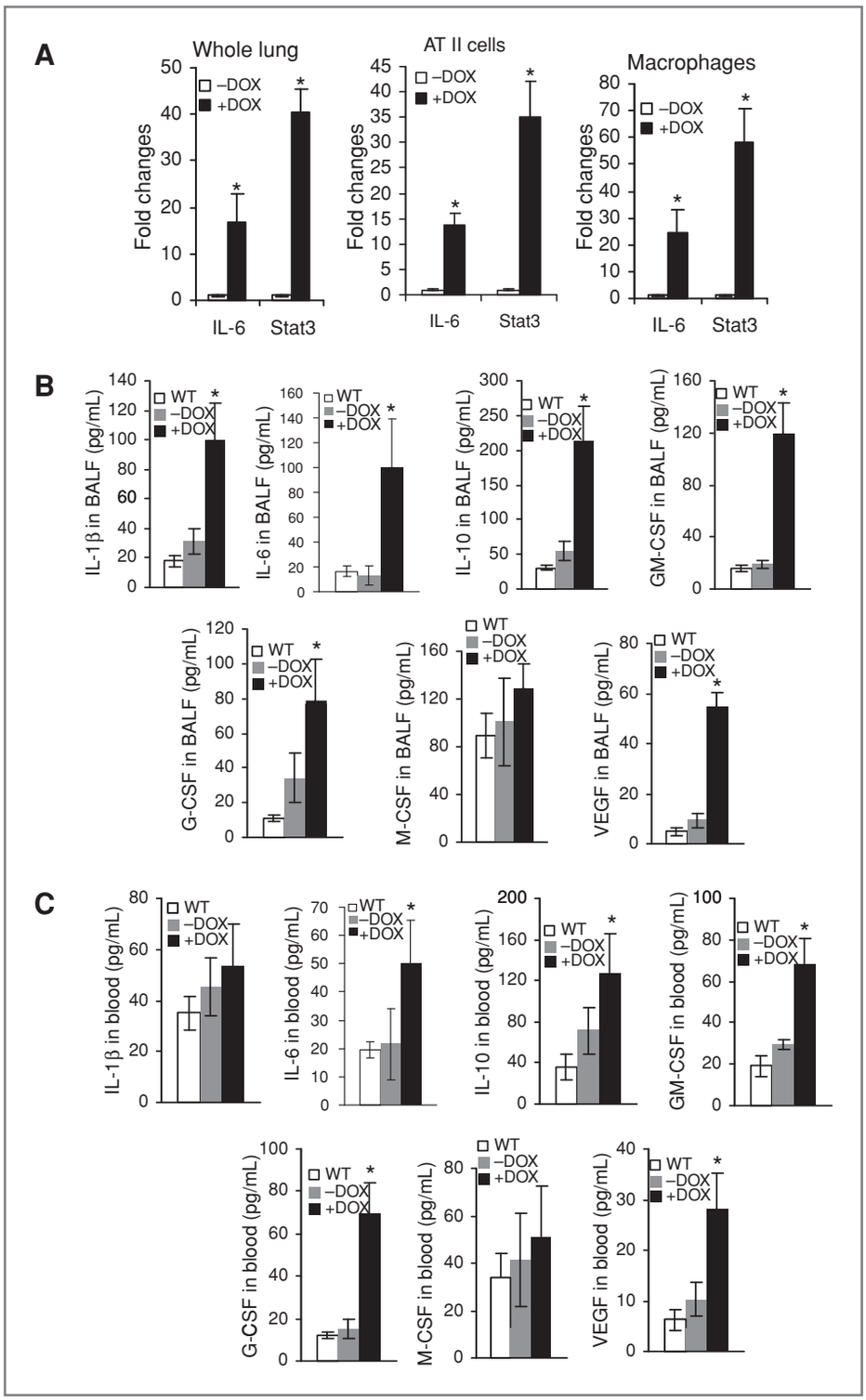

Figure 4. Upregulation of protumor cytokines in bitransgenic mice. A, real-time PCR was carried out to quantify mRNA expression levels of IL-6 and Stat3 in the whole lung, AT II epithelial cells and alveolar macrophages of 1-month doxycycline treated (+DOX) or untreated (−DOX) bitransgenic mice, and was normalized by GAPDH mRNA expression. Results represent the mean ± SD. $n = 5$. *, $P < 0.05$. B, concentrations of IL-1β, IL-6, IL-10, GM-CSF, G-CSF, M-CSF, and VEGF in BALF of wild-type (WT) mice, 3-month +DOX, or −DOX bitransgenic transgenic mice were measured by ELISA. Results represent the mean ± SD. $n = 5$. *, $P < 0.05$. C, concentrations of IL-1β, IL-6, IL-10, GM-CSF, G-CSF, M-CSF, and VEGF in the blood of WT mice, 3-month +DOX, or −DOX bitransgenic transgenic mice were measured by ELISA. Results represent the mean ± SD. $n = 5$; *, $P < 0.05$.

expansion of MDSCs was a result of myeloid differentiation originating from the bone marrow. It is intriguing to speculate that Api6 converts local macrophages to MDSCs in the lung. To test this assumption, alveolar monocytes/macrophages from 3-month-old wild-type mice were isolated from BALF and cultured *in vitro* in the presence or absence of Api6 protein for 3 days. Cultured cells were stained with anti-CD11b and anti-Ly6G antibodies, and analyzed by FACS. Interestingly, the

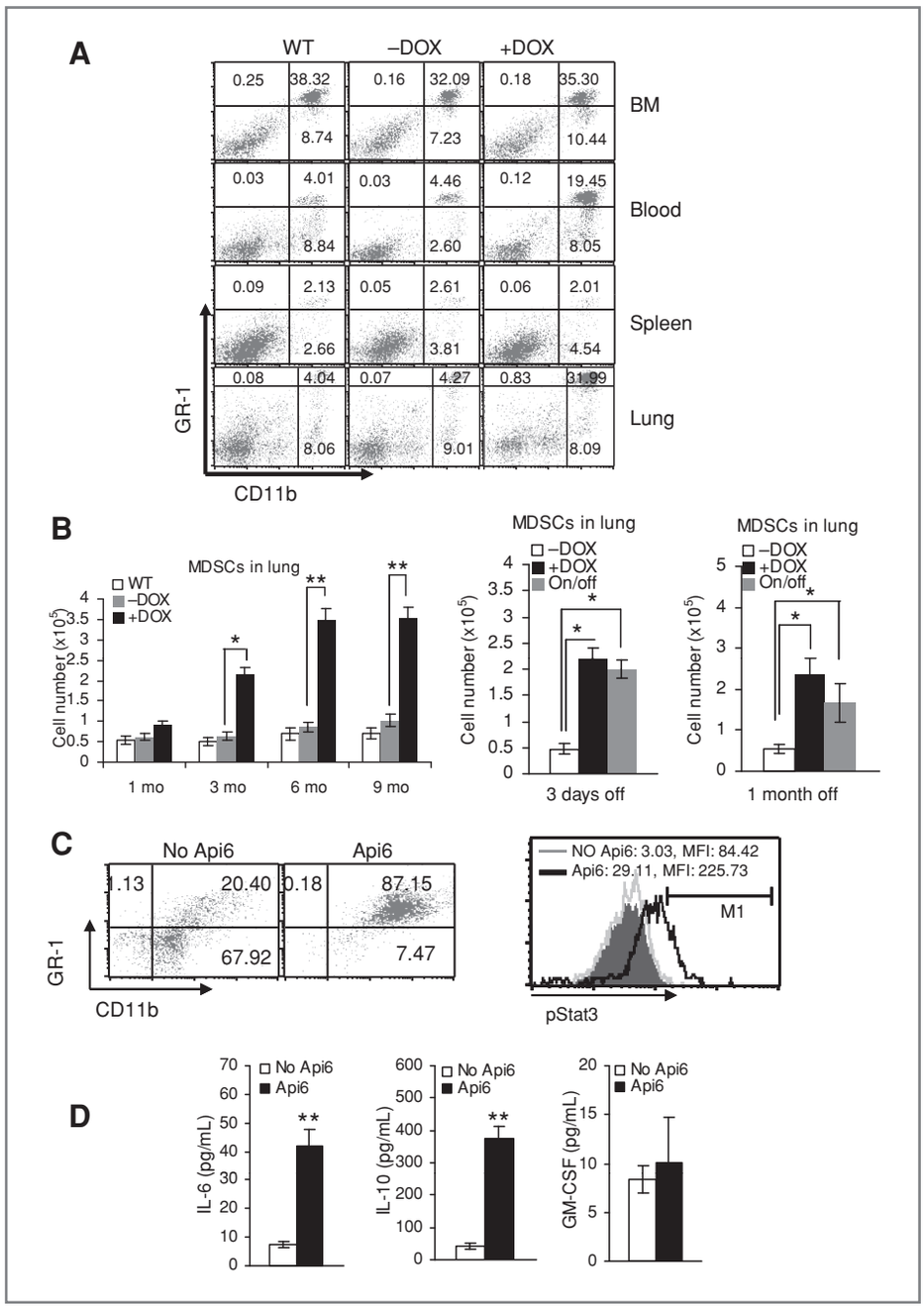

Figure 5. Api6 induced alveolar monocytes/macrophages to $CD11b^+Ly6G^+$ cell transition. A, single-cell suspensions were prepared from the bone marrow (BM), blood, spleen, and lung of 3-month doxycycline-treated (+DOX), untreated (−DOX) bitransgenic mice, and age-matched wild-type (WT) mice. The percentage of the $CD11b^+Ly6G^+$ cell population was analyzed by FACS in dot plots. B, the total numbers of the $CD11b^+Ly6G^+$ cell population in the lung were analyzed by FACS in dot plots. In separate groups, doxycycline was removed for 3 days or 1 month from bitransgenic mice followed by FACS analysis. Results represent the mean ± SD. $n = 5$; *, $P < 0.05$. C, alveolar macrophages from 3-month-old WT mice were cultured *in vitro* in the presence or absence of Api6 for 2 days. Cultured cells were stained with anti-CD11b antibody, anti-Ly6G antibody, and phospho-Stat3Y705 antibody for FACS analysis. Left, the percentage of the $Ly6G^+CD11b^+$ cell population in dot plots. Right, the percentage and the mean fluorescence intensities (MFI) of phospho-Stat3 in $CD11b^+Ly6G^+$ cells in histogram.
D, concentrations of IL-6, IL-10, and GM-CSF in the supernatants of above cultured cells were measured by ELISA. Results represent the mean ± SD. $n = 5$. *, $P < 0.05$; **, $P < 0.01$.

percentage of $CD11b^+Ly6G^+$ myeloid cells was significantly increased in the Api6-treated group (87.15%) compared with those in the untreated group (20.40%; Fig. 5C). The phosphorylated Stat3 level was dramatically increased in $CD11b^+Ly6G^+$ myeloid cells of the Api6-treated group (Fig. 5C), which is a characteristic of MDSCs *in vivo* (Supplementary Table S1). Furthermore, concentrations of IL-6, IL-10, and GM-CSF were dramatically increased in the culture medium of the Api6-treated group (Fig. 5D). This observation clearly suggests that Api6 can convert regional macrophages to MDSCs.

$CD11b^+Ly6G^+$ lung MDSCs suppress T-cell proliferation and function *in vitro*

Next, it was important to show whether $CD11b^+Ly6G^+$ myeloid cells from the bitransgenic lung possess an immunosuppressive function. Carboxyfluorescein succinimidyl ester (CFSE)-labeled wild-type $CD4^+$ T cells were stimulated with anti-CD3 monoclonal antibody (mAb) plus anti-CD28 mAb for 3 days and cocultured with lung $CD11b^+Ly6G^+$ myeloid cells (MDSC:T cell ratio = 1:5) *in vitro*. $CD11b^+Ly6G^+$ myeloid cells from the lung of wild-type and doxycycline-untreated bitransgenic lung lacked an inhibitory effect on

T-cell receptor–stimulated proliferation of wild-type $CD4^+$ T cells. In contrast, $CD11b^+Ly6G^+$ myeloid cells from the lung of doxycycline-treated bitransgenic mice showed complete inhibition on proliferation of wild-type $CD4^+$ T cells (Fig. 6A). This was further confirmed by a significant reduction of CD69 expression on $CD4^+$ T cells, a key molecular marker for T-cell activation (Fig. 6B). Functionally, secretion of T-cell lymphokines, including IL-2, IL-4, and IFN-γ was also reduced in the coculturing medium with $CD11b^+Ly6G^+$ myeloid cells from doxycycline-treated bitransgenic mice (Fig. 6C), an implication of functional impairment. To further determine whether the inhibition of T-cell proliferation was secondary to apoptosis, Annexin V analysis was carried out in which wild-type $CD4^+$ T cells were stained with Annexin V antibody after coculture with various $CD11b^+Ly6G^+$ myeloid cells. $CD4^+$ T cells showed the highest apoptotic activity when cocultured with $CD11b^+Ly6G^+$ myeloid cells from the lung of doxycycline-treated bitransgenic mice (Fig. 6D). There was no distinctive apoptotic activity of $CD4^+$ T cells after coculturing with $CD11b^+Ly6G^+$ myeloid cells from the lung of wild-type or

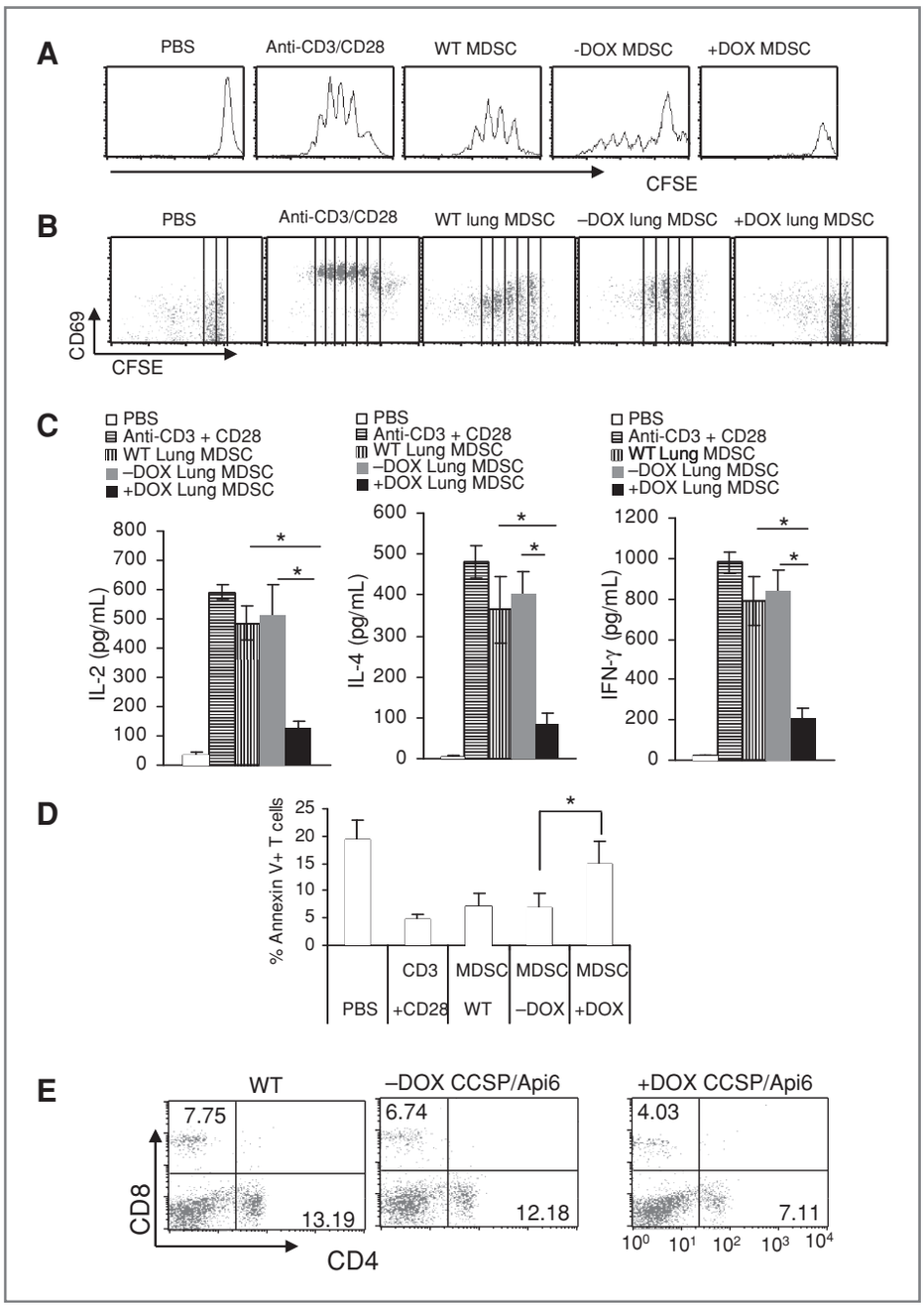

Figure 6. Immune suppression in bitransgenic mice. A, CFSE-labeled wild type splenic $CD4^+$ T cells were stimulated with anti-CD3 mAb plus anti-CD28 mAb for 4 days in the presence or absence of MDSCs from the lung of wild type (WT MDSCs), 3-month doxycycline-treated (+DOX MDSCs) or untreated (−DOX MDSCs) bitransgenic mice. The ratio of MDSC/$CD4^+$ T cell was 1:5. Proliferation of labeled $CD4^+$ T cells was analyzed as CFSE dilution by FACS. Peaks represent cell division cycles. PBS was negative control. Anti-CD3 plus anti-CD28 without MDSCs was positive control. B, CFSE-labeled $CD4^+$ T cells were cocultured with MDSCs as above. After 72 hours, cocultured cells were stained with anti-CD69 and CD4 antibodies for FACS analysis. In gated $CD4^+$ T cells, a representative histogram of CD69/CFSE double-positive cells was shown. C, the concentrations of IL-2, IL-4, and IFN-γ in the above cultured medium were measured by ELISA. Results represent the mean ± SD. $n = 5$. *, $P < 0.05$; D, WT $CD4^+$ T cells were cocultured with MDSCs as described in A and labeled with Annexin V and anti-CD4 antibodies for FACS analysis. Results represent the mean ± SD. $n = 5$; *, $P < 0.05$. E, single-cell suspensions were prepared from the lung of 3-month +DOX, −DOX bitransgenic mice, and age-matched WT mice. The percentage of the $CD4^+$ and $CD8^+$ cell populations was analyzed by FACS in dot plots.

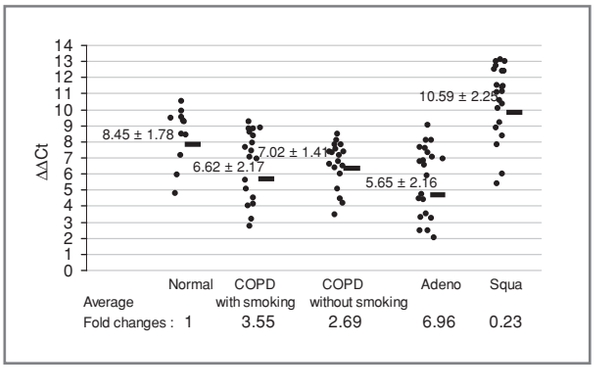

Figure 7. Api6 upregulation in human tumor and COPD. Real-time PCR was carried out to quantify mRNA expression levels of Api6 in human lung tissues from adenocarcinoma (Adeno), squamous cell carcinoma (Squa), and COPD patients, and normalized by GAPDH mRNA expression. Numbers in each column represent average ΔCt. Average fold changes were determined by $2^{(\Delta\Delta Ct)}$, in which ΔΔCt = ΔCt (cancer or COPD samples) − ΔCt (normal human samples). Numbers on the bottom represent average fold changes compared with the normal human samples. Normal human samples were set up as 1.

doxcycline-untreated bitransgenic mice. As a consequence, decreased $CD4^+$ and $CD8^+$ T-cell populations were observed in the doxcycline-treated bitransgenic lung compared with those in the lungs of wild-type or untreated mice (Fig. 6E).

Api6 upregulation in human COPD and adenocarcinoma

Because Api6 overexpression caused emphysema and lung tumor formation in the CCSP-rtTA/$(TetO)_7$-CMV-Api6 bitransgenic mouse model, it is intriguing to determine whether upregulation of Api6 is associated with lung cancer and COPD in humans. The expression level of Api6 mRNA in human adenocarcinomas ($n = 21$), squamous cell carcinomas ($n = 20$), COPD without smoking ($n = 18$), and COPD with smoking ($n = 18$) versus normal samples ($n = 12$) were examined by quantitative real-time PCR (Fig. 7). In comparison with normal human lungs, the average of Api6 mRNA expression levels was 6.96-fold higher in adenocarcinomas, 2.69-fold higher in lung tissues with COPD from nonsmokers, and 3.55-fold higher in lung tissues with COPD from smokers. However, the average of Api6 mRNA expression levels was 0.23-fold lower in squamous cell carcinomas, compared with those in normal human lung groups.

Discussion

Here, we present data that Api6 possesses dual functions in controlling both epithelial cancerous transformation and expansion of MDSCs. Api6 overexpression in AT II epithelial cells of bitransgenic mice blocked the apoptotic pathway, promoted epithelial cell proliferation (Fig. 2), and induced emphysema/hypercellularity (Fig. 3), similar to those observed in $lal^{-/-}$ mice (3). In short-term doxycycline removal studies (3 days), the apoptotic activities and proinflammatory cytokine concentrations in the lung were not reversed in the lung (Supplementary Fig. S1A and B). Even in the long-term doxycycline removal studies (1 month), the apoptotic activities and proinflammatory cytokine concentrations in the lung were not completely reversed to the normal levels in the lung (Supplementary Fig. S2A and B). After stopping treatment of doxycycline for 1 month, hyperplasia still existed in the lung (Fig. 3E). It seems that once proinflammatory cytokines are upregulated by Api6, they sustain the neoplastic process even in the absence of Api6. Subsequently, adenocarcinoma was developed in the lung at a 40% rate after 3 to 4 months of doxycycline treatment (Fig. 3B). This is different from the fast-growing and fast-regressing lung tumor mouse models, in which lung tumors can be induced quickly upon doxycycline treatment and regress quickly after doxycycline removal (19–21). Our model resembles the smoking population in humans, in which smokers still develop lung cancer even after stopping smoke. We made a similar observation in another CCSP-rtTA/$(TetO)_7$-CMV-MMP12 bitransgenic mouse model (11).

Activation of oncogenic intracellular Stat3, Erk, Akt, and P38 signaling in AT II epithelial cells was involved in the Api6-induced pathogenic process (Supplementary Table S1). As reported previously, persistent activation of Stat3 and Kras (upstream regulator of Erk and P38) in AT II epithelial cells was able to induce lung tumor (10, 19). Therefore, Api6 overexpression caused AT II epithelial cells to induce cancerous transformation at least by 2 mechanisms, blocking apoptosis and activating oncogenic pathways.

Api6 overexpression in AT II epithelial cells also showed immunomodulatory activity. It promoted $CD11b^+Ly6G^+$ myeloid cell expansion in the lung and blood (Fig. 5A and B). Interestingly, removal of doxycycline did not result in a decrease in the number of MDSCs in the lung (Fig. 5B). Because the bone marrow and spleen were not affected (Fig. 5A and B), $CD11b^+Ly6G^+$ myeloid cell expansion in the lung was unlikely due to a hematopoietic abnormality as we reported recently (22). The regional $CD11b^+Ly6G^+$ myeloid cell expansion must be due to a local effect caused by Api6 overexpression in the bitransgenic lung. This was tested directly in an *in vitro* experiment. The purified Api6 protein stimulated *in vitro* cultured wild-type alveolar monocytes/macrophages to $CD11b^+Ly6G^+$ myeloid cell transition (Fig. 5C). This interesting observation for the first time showed a reverse process of myeloid cells from a more mature stage back to an immature stage under pathogenic condition. Importantly, *in vitro* converted $CD11b^+Ly6G^+$ myeloid cells showed characteristics of MDSCs, including increased activation of Stat3 (Fig. 5C) and increased secretory levels of IL-6, IL-10, and GM-CSF that are known to be secreted by MDSCs in cultured medium (Fig. 5D). When cocultured *in vitro*, $CD11b^+Ly6G^+$ myeloid cells isolated from doxycycline-treated bitransgenic mice inhibited wild-type $CD4^+$ T-cell proliferation and function (Fig. 6).

Api6 also induce lung inflammation and adenocarcinoma through a myeloid-initiated mechanism as we reported previously (12). Compared with the regional inflammation in CCSP-rtTA/$(TetO)_7$-CMV-Api6 bitransgenic mice, Api6 overexpression in myeloid cells led to systemic inflammation in cfms-rtTA/$(TetO)_7$-CMV-Api6 bitransgenic mice. It promoted expansion of MDSCs in multiple organ compartments starting from the bone marrow by both inhibiting apoptosis and

stimulating proliferation of myeloid lineage cells. MDSCs in all compartments showed strong activation of Stat3, Erk, and P38. We also reported that activation of these oncogenic molecules served as hallmarks for MDSCs in other animal models (6, 11, 12). In cfms-rtTA/$(TetO)_7$-CMV-Api6 bitransgenic mice, infiltration of Api6-induced MDSCs into the lung changed the local microenvironment and promoted adenocarcinoma (12). In a paracrine fashion, Api6 secreted from myeloid cells stimulated epithelial cells to cancerous transformation. Interactions among different cell types by paracrine and autocrine mechanisms triggered by Api6 overexpression in epithelial cells or myeloid cells synergize cell–cell interaction and proliferation.

During characterization of multiple inflammation-triggered lung spontaneous tumor animal models, we noticed that a group of genes were always upregulated/activated together during tumorigenesis. This supports a concept that a protumor network exists in the body to coordinate inflammation and lung adenocarcinoma formation. More studies are needed to identify members in this network and elucidate their relationships with lung adenocarcinoma, as these molecules can potentially serve as biomarkers for lung cancer diagnosis/prediction and therapeutic targets. We are particularly interested in secretory proteins (e.g. Api6) as they can be used for blood and BALF screening in cancer patients. In Figure 7, Api6 mRNA was increased in human COPD and adenocarcinoma, but was decreased in squamous cell carcinoma by real-time PCR analysis. Previously, we reported that another LAL downstream gene MMP12 also induced emphysema and lung tumorigenesis when it is overexpressed in AT II epithelial cells through a similar MDSCs and immunosuppressive mechanism (11). When tested in humans, MMP12 mRNA was increased in COPD, adenocarcinoma, and squamous cell carcinoma (11). Through studying CCSP-rtTA/$(TetO)_7$-CMV-Stat3C bitransgenic mice, multiple Stat3 downstream genes were identified to be associated with COPD/emphysema and lung cancer in animals and humans (10, 23). In the future, characterization of these proteins will facilitate identification of new members in the cancer promoting network of the lung.

Disclosure of Potential Conflicts of Interest

No potential conflicts of interest were disclosed.

Acknowledgments

The authors thank Dr. Rebecca A. Shilling for critical reading of the manuscript.

Grant Support

This study was supported by NIH grants HL087001 (H. Du); CA138759 (C. Yan); and HL061803 and HL067862 (C. Yan and H. Du).

The costs of publication of this article were defrayed in part by the payment of page charges. This article must therefore be hereby marked *advertisement* in accordance with 18 U.S.C. Section 1734 solely to indicate this fact.

Received November 24, 2010; revised June 14, 2011; accepted June 14, 2011; published OnlineFirst June 22, 2011.

References

1. Du H, Heur M, Duanmu M, Grabowski GA, Hui DY, Witte D, et al. Lysosomal acid lipase-deficient mice: depletion of white and brown fat, severe hepatosplenomegaly, and shortened life span. J Lipid Res 2001;42:489–500.
2. Du H, Duanmu M, Witte D, Grabowski GA. Targeted disruption of the mouse lysosomal acid lipase gene: long-term survival with massive cholesteryl ester and triglyceride storage. Hum Mol Genet 1998;7:1347–54.
3. Lian X, Yan C, Yang L, Xu Y, Du H. Lysosomal acid lipase deficiency causes respiratory inflammation and destruction in the lung. Am J Physiol Lung Cell Mol Physiol 2004;286:L801–7.
4. Lian X, Yan C, Qin Y, Knox L, Li T, Du H. Neutral lipids and peroxisome proliferator-activated receptor-{gamma} control pulmonary gene expression and inflammation-triggered pathogenesis in lysosomal acid lipase knockout mice. Am J Pathol 2005;167:813–21.
5. Yan C, Lian X, Li Y, Dai Y, White A, Qin Y, et al. Macrophage-Specific Expression of Human Lysosomal Acid Lipase Corrects Inflammation and Pathogenic Phenotypes in lal-/- Mice. Am J Pathol 2006;169:916–26.
6. Qu P, Shelley WC, Yoder MC, Wu L, Du H, Yan C. Critical roles of lysosomal acid lipase in myelopoiesis. Am J Pathol 2010;176:2394–404.
7. Gebe JA, Llewellyn M, Hoggatt H, Aruffo A. Molecular cloning, genomic organization and cell-binding characteristics of mouse Spalpha. Immunology 2000;99:78–86.
8. Miyazaki T, Hirokami Y, Matsuhashi N, Takatsuka H, Naito M. Increased susceptibility of thymocytes to apoptosis in mice lacking AIM, a novel murine macrophage-derived soluble factor belonging to the scavenger receptor cysteine-rich domain superfamily. J Exp Med 1999;189:413–22.
9. Kurokawa J, Arai S, Nakashima K, Nagano H, Nishijima A, Miyata K, et al. Macrophage-derived AIM is endocytosed into adipocytes and decreases lipid droplets via inhibition of fatty acid synthase activity. Cell Metab 2010;11:479–92.
10. Li Y, Du H, Qin Y, Roberts J, Cummings OW, Yan C. Activation of the signal transducers and activators of the transcription 3 pathway in alveolar epithelial cells induces inflammation and adenocarcinomas in mouse lung. Cancer Res 2007;67:8494–503.
11. Qu P, Du H, Wang X, Yan C. Matrix metalloproteinase 12 overexpression in lung epithelial cells plays a key role in emphysema to lung bronchioalveolar adenocarcinoma transition. Cancer Res 2009;69:7252–61.
12. Qu P, Du H, Li Y, Yan C. Myeloid-specific expression of Api6/AIM/Sp alpha induces systemic inflammation and adenocarcinoma in the lung. J Immunol 2009;182:1648–59.
13. Tichelaar JW, Lu W, Whitsett JA. Conditional expression of fibroblast growth factor-7 in the developing and mature lung. J Biol Chem 2000;275:11858–64.
14. Qu P, Du H, Wilkes DS, Yan C. Critical roles of lysosomal acid lipase in T cell development and function. Am J Pathol 2009;174:944–56.
15. Nikitin AY, Alcaraz A, Anver MR, Bronson RT, Cardiff RD, Dixon D, et al. Classification of proliferative pulmonary lesions of the mouse: recommendations of the mouse models of human cancers consortium. Cancer Res 2004;64:2307–16.
16. Gabrilovich DI, Nagaraj S. Myeloid-derived suppressor cells as regulators of the immune system. Nat Rev Immunol 2009;9:162–74.
17. Ostrand-Rosenberg S, Sinha P. Myeloid-derived suppressor cells: linking inflammation and cancer. J Immunol 2009;182:4499–506.
18. Kao J, Ko EC, Eisenstein S, Sikora AG, Fu S, Chen SH. Targeting immune suppressing myeloid-derived suppressor cells in oncology. Crit Rev Oncol Hematol 2011;77:12–9.
19. Fisher GH, Wellen SL, Klimstra D, Lenczowski JM, Tichelaar JW, Lizak MJ, et al. Induction and apoptotic regression of lung adenocarcinomas by regulation of a K-Ras transgene in the presence and absence of tumor suppressor genes. Genes Dev 2001;15:3249–62.

20. Politi K, Zakowski MF, Fan PD, Schonfeld EA, Pao W, Varmus HE. Lung adenocarcinomas induced in mice by mutant EGF receptors found in human lung cancers respond to a tyrosine kinase inhibitor or to down-regulation of the receptors. Genes Dev 2006;20:1496–510.

21. Ji H, Li D, Chen L, Shimamura T, Kobayashi S, Mcnamara K, et al. The impact of human EGFR kinase domain mutations on lung tumorigenesis and *in vivo* sensitivity to EGFR-targeted therapies. Cancer Cell 2006;9:485–95.

22. Qu P, Yan C, Du H. Matrix metalloproteinase 12 overexpression in myeloid lineage cells plays a key role in modulating myelopoiesis, immune suppression, and lung tumorigenesis. Blood 2011;117: 4476–89.

23. Qu P, Roberts J, Li Y, Albrecht M, Cummings OW, Eble JN, et al. Stat3 downstream genes serve as biomarkers in human lung carcinomas and chronic obstructive pulmonary disease. Lung Cancer 2009;63: 341–7.